Comprehensive study of nine novel cases of TFEB-amplified renal cell carcinoma: an aggressive tumour with frequent PDL1 expression

Solene-Florence Kammerer-Jacquet, Camille Gandon, Frederic Dugay, Brigitte Laguerre, Benoit Peyronnet, Romain Mathieu, Gregory Verhoest, Karim Bensalah, Xavier Leroy, Sebastien Aubert, et al.

Comperat Eva (Orcid ID: 0000-0001-8488-543X)
Florence Kammerer-Jacquet Solene (Orcid ID: 0000-0002-6623-741X)

Comprehensive study of 9 novel cases of *TFEB*-amplified renal cell carcinoma: an aggressive tumor with frequent PDL1 expression

Solène-Florence Kammerer-Jacquet[1-2*], Camille Gandon[1*], Frederic Dugay[2-3], Brigitte Laguerre[4], Benoit Peyronnet[5], Romain Mathieu[5], Grégory Verhoest[5], Karim Bensalah[5], Xavier Leroy[6], Sebastien Aubert[6], Catherine Vermaut[7], Fabienne Escande[7], Virginie Verkarre[8], Eva Compérat[9], Damien Ambrosetti[10], Florence Pedeutour[11], Marc-Antoine Belaud-Rotureau[2-4], Nathalie Rioux-Leclercq[1-2]

and the members of CARARE French network (Rare Renal Carcinoma in Adults) of the INCa (National Institut of Cancer, France).

[1]Department of Pathology, University Hospital, Rennes, France; [2]UMR 6290-IGDR, Rennes, France; [3]Department of Cytogenetics, University Hospital, Rennes, France; [4]Department of Oncology, Eugène Marquis Centre, Rennes, France; [5]Department of Urology, University Hospital, Rennes, France; [6]Univ.Lille, CHU Lille, Department of Pathology, F-59000, Lille, France; [7]Department of Biochemistry and Molecular Biology, University Hospital, Lille, France; [8]Department of Pathology, HEGP, AP-HP-centre, Paris University, Paris, France; [9]Department of Pathology, Tenon, AP-HP, Paris, France; [10]Department of Pathology, University Hospital, Nice, France; [11] Laboratory of Solid Tumor Genetics, University Hospital of Nice-Côte d'Azur University, Institute for Research on Cancer and Aging of Nice (IRCAN), CNRS UMR 7284/INSERM U1081, Nice, France.

* These authors contributed equally to the work and are considered as first co-authors.

Corresponding author:

Solene-Florence Kammerer-Jacquet

Service d'Anatomie Pathologique, CHU Pontchaillou

2 rue Henri Le Guilloux

35 033 Rennes cedex 9

This article has been accepted for publication and undergone full peer review but has not been through the copyediting, typesetting, pagination and proofreading process which may lead to differences between this version and the Version of Record. Please cite this article as doi: 10.1111/his.14683

Telephone number: 0033 2 99 28 42 79

Fax number: 0033 2 99 28 42 84

Email address: soleneflorence.kammerer-jacquet@chu-rennes.fr

Disclosure of potential conflicts of interest:

The authors of this article have no relevant financial relationships with commercial interests to disclose and no funding to declare.

Running head: TFEB-amplified renal cell carcinoma

Word count: 2487

ABSTRACT

Background & objectives: First described in 2014, renal cell carcinoma (RCC) with *TFEB* amplification (6p21) is a rare molecular subgroup whose diagnosis is challenging. The prognosis and therapeutic implications remain unclear.

Methods: We report here the clinical, histological, immunohistochemical and genetic features of 9 novel cases. The pathological and immunohistochemical features were centrally reviewed by expert uropathologists. Fluorescence in situ hybridization (FISH) confirmed the diagnosis and comparative genomic hybridization (CGH) was performed to determine quantitative genomic alterations. We also performed an exhaustive review of the literature and compiled our data.

Results: *TFEB*-amplified RCC were locally advanced with initial lymph node involvement in one case and liver metastasis in another case. They were high-grade eosinophilic tumors with papillary/pseudopapillary architecture, frequent positivity for melanocytic markers and frequent PDL1 expression. FISH demonstrated high-level *TFEB* amplification in 6 cases. One case showed concomitant *TFEB* translocation. CGH analysis identified complex alterations with frequent losses of 1p, 2q, 3p, 6p, and frequent 6p and 8q gains. *VEGFA* co-amplification was identified in all cases with a lower level than TFEB. The prognosis was poor with five patients having lymph node or distant metastases.

Conclusion: *TFEB*-amplified RCC is a rare molecular subgroup with variable morphology whose diagnosis is confirmed by FISH analysis. The complex alterations identified by CGH are consistent with an aggressive clinical behavior. The co-amplification of *VEGFA* and the expression of PDL1 could suggest a potential benefit from antiangiogenics and targeted immunotherapy in combination for these aggressive tumors.

Keywords : renal cell carcinoma ; TFEB gene ; amplification ; MITF

INTRODUCTION

Historically, renal cell carcinoma (RCC) classification was mainly based on morphology (1). Over the past few years, genetic aberrations have contributed to define new entities (2). Microphthalmia transcription factor family (MITF) translocation RCC is now considered as a separate entity among RCC in the current 2016 WHO Classification of Tumors of the Urinary System (1). Four transcription factors are described as members of this family: *MITF, TFEC, TFEB* and *TFE3*. The rearrangement of *TFE3* (Xp11) and *TFEB* (6p21) have been involved in the development of RCC (3). *TFE3* translocated RCC are found in about 20-40% of pediatric and 1-4% of adult RCC (4,5), whereas *TFEB* translocated carcinomas are very rare with approximatively one hundred cases reported in the literature (6).

TFEB plays an important role in organelle biogenesis and metabolic processes. In particular, it participates to the regulation of lysosomal biogenesis, lysosomal acidification, lysosomal exocytosis, endocytosis, autophagy and membrane repair (7). Recently, TFEB dysregulation was found to play a crucial pathogenic role in different tumors by modulating tumor cell autophagy (8). Because autophagy is activated in hypoxic areas of tumors in order to maintain cancer cell growth (9), it is not surprising that overexpression of TFEB potentiates its intrinsic pro-oncogenic activity (10).

In the vast majority of *TFEB* translocated RCC, the partner is *MALAT1* (11q12) (which has a stronger promoter resulting in the overexpression of TFEB (11,12, 13). This entity was initially described in 2001 (14). It is classically composed of nests of epithelioid cells with clear to eosinophilic cytoplasm, associated with a subpopulation of smaller cells surrounding hyaline basement membrane material (15). Despite an epithelioid morphology, these tumors under express epithelial markers and PAX8 relative to typical RCC (16). However, they frequently express melanocytic markers such as Melan-A and HMB45 that are downstream targets of TFEB (14). A frequent expression of PDL1 was recently described (17).

Because TFEB is supposed to drive oncogenesis in this molecular subgroup, other mechanisms increasing its expression, such as amplification, could generate a similar phenotype. Several studies have reported cases of *TFEB*-amplified RCC that share in common with *TFEB*-translocated RCC the expression of TFEB and downstream targets HMB45 and Melan-A but with morphological discrepancies and a worse clinical prognosis for *TFEB*-amplified RCC (18-33).

Here, we report 9 novel cases, with clinical, morphological, immunohistochemical (PDL1 status for the first time) and genomic features. We also performed an exhaustive review of the literature and confronted our data with the previously reported cases.

METHODS

Patients' selection

Patients originated from Rennes University Hospital or others French medical centers. Most of them were addressed for second opinion. They were all included in the French CARARE network (Rare Renal Cancer in Adults) of the INCa (National Institute of Cancer, France), which focuses on rare subtypes of RCC or RCC occurring in young people (≤ 40 years). All procedures were performed in accordance with the ethical standards of the Helsinki Declaration. The study was approved by the Ethical Committee (CNIL DR-2013-206).

Pathological analysis

Fresh surgical specimens were received at the departments of Pathology and tumors were described at gross examination. Samples were formalin fixed and paraffin embedded with hematoxylin and eosin-safran staining (HES). The HES slides were addressed for second opinion and then centrally reviewed by two uropathologists (NRL and SFJK).

Immunohistochemistry

Four-µm thick whole tissue sections were cut and mounted on glass slides (Superfrost+, Menzel Gläser, Thermo Fisher Scientific, Waltham, Massachusetts, USA). The preparations were dried for 1 hour at 58°C, and then overnight at 37°C. The sections were deparaffinized with toluene and rehydrated with ethanol. The preparations were pretreated and immunostained using Ventana Benchmark XT, Ventana Medical Systems, Oro Valley, Arizona, USA. Immunohistochemical analyses were carried out using the following antibodies: anti-PAX8 (clone MRQ50, Ventana Medical Systems), anti-CD117 CKit (monoclonal, Ventana Medical Systems), anti-Melan-A (clone A103, Ventana Medical Systems), anti-HMB45 (monoclonal,

Dako, Agilent, Santa Clara, California, USA), anti-CD10 (monoclonal, Leica, Wetzlar, Germany), anti-CKAE1-AE3 (clone PCK26, Ventana Medical Systems), anti-CAIX (Abcam, Cambrige, UK), anti-CK7 (monoclonal, Dako, Agilent), anti-AMACR (monoclonal, Dako, Agilent), anti-TFE3 (Cell Marque Corporation, Rocklin, California, USA), anti-PDL1 (28-8 clone, Dako, Agilent Technologies), anti-PD1 (Dako, Agilent Technologies) and CD8 (clone C8/144B, Dako, Agilent Technologies). The clone 28-8 was choosen because it is the companion testing of Novolumab with a good reproductibility with 22C3 the companion of Pembrolizumab also widely used in RCC (34, 35). The detection was performed using horseradish peroxidase-labeled polymer conjugated secondary antibodies using diaminobenzidine as chromogen (Sigma-Aldrich, Saint Louis, Missouri, USA). The PD1 and CD8 expressions were semi-quantitatively assessed with either absent (0), low (1), moderate (2) or high (3) infiltrate as previously described (31). The tumor expressions of each antibody were independently evaluated by 2 uropathologists (NRL and SFJK). Negative controls were performed by omitting the primary antibody.

Fluorescence in situ hybridization (FISH)

FISH analysis was performed as previously described (36). Briefly, the 5-µm thick, paraffin-embedded sections fixed on slides were deparaffinized and pre-treated using pre-treatment solution (Dako). Pepsin solution was added on preparations for 6 minutes (Sigma, 100 mg/l) and then dehydrated in ethanol 70°, 85°, and 100° (2 minutes each). Specimens and probes were codenatured (10 minutes at 75°C +/-2°C) and hybridized overnight at 37°C. The *TFEB* gene status was assessed using the *TFEB* Break apart Probe 6p21.1 (Empire Genomics, Buffalo, United States). After hybridization, slides were washed according to the manufacturers' instructions, and the nuclei were counterstained by DAPI (Dako). Cells were viewed using a fluorescent Axioplan II microscope (Zeiss, Le Pecq, France) or the automatized microscope Bioview Encore (Bioview, Rehovot, Israel) with appropriate filters and 100 non-overlapped nuclei were analysed for each tumor by 2 independents observers (FD and MABR). According to the definition set by Gupta and al (24), a low-level amplification was defined by 5-10 copies and a high-level amplification by more than 10 copies.

Comparative Genomic Hybridization array study (CGH)

Copy number alterations were analyzed by array-CGH using the standard version of Agilent Human Genome CGH microarray 180K (Agilent Technologies, Santa Clara, CA, USA) according to the manufacturer's instructions. Microarrays were scanned using the Agilent G2565BA Microarray Scanner System. The images were extracted using Agilent Feature Extraction software, and data were analyzed with Agilent Cytogenomics v.2.5.8.11 software to identify chromosome imbalances.

Review of the literature

We exhaustively gathered all the published cases of *TFEB*-amplified RCC and noted their clinical, pathological and molecular details. We used Mann-Whitney test and χ^2 or Fisher's exact test to compare if there were significant differences within subgroups (between *TFEB*-amplified RCC with low or high-level amplification, and between *TFEB*-amplified RCC with or without concomitant translocation).

RESULTS

Clinical features

The clinical features of the 9 patients of our cohort are detailed in Table 1. They were adults with a male predominance (n=7, 78%), with an age range from 31 years to 86 years (mean: 60 years). The tumors presented at variable stages, from pT1a to pT3b with a majority of pT3 (n=6, 67%), with a size ranging from 3 cm to 20 cm. A majority of patients presented with metastasis, located in distant lymph nodes, liver, lungs, adrenal gland and bone at the diagnosis or during the follow-up. The delivered therapies were sunitinib, cabozantinib, mTOR inhibitor or nivolumab. The 2 patients treated by sunitinib showed progression, while no recurrence was observed after the introduction of nivolumab (after 2 and 5 months of treatment). The non-metastatic patients were free of recurrence at 18 months and 24 months.

Morphologic features

The morphologic features are illustrated in Figure 1 and detailed in Table 2. The type of architecture was variable with papillary, trabecular, alveolar and solid patterns. The cytoplasm were either eosinophilic or

clear. High-grade features such as prominent nucleoli and necrosis were frequently observed, but no sarcomatoid component. No case showed the biphasic appearance of the *TFEB*-translocated RCC. The diagnosis originally mentioned were papillary RCC, oncocytoma and clear cell RCC, Table 2.

Immunohistochemistry

The immunohistochemical results are illustrated in Figure 2 and presented in Table 3. All cases demonstrated immunoreactivity for AMACR and for PAX8. Whereas all cases expressed Melan A, only 5 of them (56%) expressed HMB45 with only focal expression. Misleading to a differential diagnosis, 4 cases (44%) focally expressed CK7, 6 cases (67%) expressed membranous CA-IX and 4 cases (44%) expressed CD117. No cases demonstrated expression of TFE3. We observed a membranous staining for PDL1 in tumor cells in 6 out of 7 samples tested (86%) with a mean percentage of 32% (5-80%). The immune infiltrate assessed with CD8 was variable but a positivity for PD1 was observed in all cases.

FISH

FISH results are illustrated in Figure 3 and detailed in Table 4, along with CGH results. All cases included in the study showed amplification of *TFEB* with a high level in 6 cases. One of the cases demonstrated both *TFEB* amplification and rearrangement. As expected, no rearrangement of *TFE3* was identified.

CGH

The gains and losses are gathered in Table 5. A profile is presented in Figure 3. Most frequents gains were identified on chromosomes 6 (78%), 8 (56%), 1 and 17 (33%) and the most frequent losses impacted chromosomes 1, 2, 6 (78%), 18 (67%), 5 including VHL (56%), 13, 19, 22 (44%), 8, 9, 17 (33%). Moreover, *VEGFA* was found co-amplified with *TFEB* in all cases but always with a lower level than *TFEB*.

Review of the literature

To the best of our knowledge, 73 cases of *TFEB*-amplified RCC have been previously reported (15-33). Including our cases, the mean age was 63 years with a male predominance. The size of the tumors ranged from 1.8 cm to 19.5 cm (mean 9 cm). Most patients presented aggressive tumors with advanced stage and

frequent metastases, Supplementary data Table 1. Most *TFEB*-amplified RCC share high grade features, with prominent nucleoli and necrosis. They exhibited variable morphology with a tubulopapillary, pseudo-papillary or nested architecture and large eosinophilic cells, Supplementary data Table 2. They frequently expressed melanocytic markers, with a frequent expression of Melan-A and a more variable expression of HMB45, Supplementary data Table 3. A majority of the reported cases showed high-level amplification, Supplementary data Table 4. Concerning the genomic profile of *TFEB*-amplified RCC, data were rather limited, Supplementary data Table 5. The more frequent gains remained on chromosome 6 and losses on chromosomes 1, 2, 3 and 6. No significant differences between *TFEB*-amplified RCC with low or high-level of amplification were identified with the exception of Melan-A positivity less expressed in TFEB low-amplified RCC ($p<0.01$), Supplementary data Table 6. Moreover, we found 11 cases with concomitant *TFEB*-amplification and translocation. None of them demonstrated the biphasic morphology usually seen in *TFEB*-translocated RCC. The RCC with both TFEB translocation and amplification did not present significant clinical or pathological differences Supplementary data Table 7.

DISCUSSION

We reported 9 novel cases of *TFEB*-amplified RCC with detailed immunohistochemical including for the first time PDL1 status and chromosomic profiles. We compared them to the previously published cases.

Our study confirms the emerging data suggesting that *TFEB*-amplified RCC occurs in older patients than TFEB-translocated RCC and demonstrates variable morphology (although frequently papillary) with high grade features. None of the cases showed the biphasic morphology classically seen in *TFEB*-translocated RCC (15). The expression of melanocytic markers is essential to the diagnosis, with a frequent expression of Melan-A and a more variable expression of HMB45. Those markers are downstream targets of TFEB, and are therefore correlated with its degree of expression. Indeed, they are more consistently expressed in *TFEB*-translocated RCC, which has a higher TFEB expression (32). This explained that Melan-A was significant less expressed in low- level amplification than in high-level *TFEB*-amplification. The diagnosis of

this new molecular subgroup relies on FISH, demonstrating an amplification of *TFEB*. Rarely, a concomitant translocation of *TFEB* can be found but this does not seem to confer any clinical, or immunohistochemical particularities, within the limit of a low number of cases. The clinical course is usually aggressive, contrary to *TFEB*-translocated RCC, which is frequently indolent. When the 2 events are present, the tumor is therefore classified as *TFEB*-amplified RCC. The chromosomic profile show many alterations, which correlates with a poor prognosis. No specific genomic pattern was identified contrary to other entities (2, 37), which highlights the driving role played by TFEB in the oncogenesis.

The differential diagnosis of a *TFEB*-amplified RCC mainly include clear cell RCC, papillary RCC, oncocytoma/chromophobe RCC and *TFE3/TFEB*-translocated RCC. First, the solid or trabecular architecture associated with clear and eosinophilic cytoplasm and prominent nucleoli raises the differential diagnosis of clear cell RCC, which frequently shows cells with eosinophilic cytoplasm in high grade tumors (38). The positivity of carbonic anhydrase 9 (CA-IX) could be misleading and needs to be interpreted with caution especially next to necrosis. Also, the deletion of *VHL* is not uncommon but no *VHL* mutations were identified. Secondly, the papillary architecture as well as the positivity for AMACR could argue for the differential diagnosis of papillary RCC so as the gains in chromosomes 7 and 17 that can be identified by FISH. Furthermore, the eosinophilic tumor cells could raise the diagnosis of oncocytoma or chromophobe RCC.

However, the prominent nucleoli in *TFEB*-amplified RCC are not in favor of these diagnoses. The differential diagnosis with *TFE3* and *TFEB*-translocated RCC is difficult as they demonstrate variable morphology, even though the biphasic pattern is more specific of the last entity. The key to the diagnosis of *TFEB*-amplified RCC is the expression of melanocytic markers that we suggest to perform in every unclassified RCC. FISH analysis is required to confirm *TFEB* amplification.

Genomic amplification is a very rare event in RCC, even less frequent than translocation (39). Recent studies have been focusing on *TFEB*, which is implicated in mTORC1 pathway, a key to the oncogenesis of many cancers. TFEB is an important regulator of lysosomal biogenesis and autophagy, and its activity is inhibited by mTORC1 to promote anabolic pathways (7, 40-44). The overexpression of TFEB influences

mTORC1 as well by increasing its activation (45). In addition, *TFEB* amplification is often combined with amplification of *VEGFA* (24), but with a lower number of copies than for *TFEB* (29), suggesting that *TFEB* rather than *VEGFA* drives the oncogenesis. However, amplifications of *VEGFA* have been associated with a poor prognosis (24, 46). Indeed, *VEGFA* has a well know angiogenic effect on endothelial cells, leading to increased tumor growth despite hypoxia. Moreover, emerging data show that *VEGFA* may also have an autocrine effect on tumors cells with the subsequent activation of the AKT/mTOR signalling pathway (47). The amplification of both *TFEB* and *VEGFA* could have a synergic effect through mTOR signaling pathway. Consequently, mTOR inhibitors and antiangiogenics could be proposed. Indeed, many patients received a treatment with mTOR inhibitors, but generally with a poor response (19,22,24,25). On this point, a study showed that TFEB induced PDL1 expression, and this could mediate resistance to mTOR inhibition (48). In this study, we assessed PDL1 status along with quantification of the immune infiltrate and demonstrate that a vast majority of cases showed positivity. This suggests the use of immunotherapies alone or in combination with mTOR inhibitors or antiangiogenics. A few patients received nivolumab, with promising results, although long-term data were very limited. Collective efforts are needed to reach optimal treatment in this very rare molecular subgroup.

In conclusion, we strongly recommend the use of melanocytic markers in unclassified RCC to detect *TFEB*-amplified RCC that need to be confirmed by FISH analysis. The diagnosis of this molecular subgroup is important because the tumors are particularly aggressive. Additional studies are needed to define the best treatment strategy.

Acknowledgements

The authors would like to thank the members of CARARE French network and the French Institute of Cancer (INCa) for their financial support. The contribution of each author was redaction of the paper (SFKJ, CG), interpretation of the data (FD, NRL, MABR, SA, CV, FP, DA, XL, FE, VV, EC) and the collection of data (BL, BP, RM, KB). All authors edited the manuscript. The authors would also like to thank Pascale Bellaud and Roselyne Viel from the Histopathology platform H2P2-BIOSIT at the Faculty of Medicine in Rennes for their technical support.

Data availability statement

The data that support the findings of this study are available on request from the corresponding author. The data are not publicly available due to privacy or ethical restrictions.

REFERENCES

1. Moch H, Cubilla AL, Humphrey PA, Reuter VE, Ulbright TM. The 2016 WHO Classification of Tumours of the Urinary System and Male Genital Organs-Part A: Renal, Penile, and Testicular Tumours. Eur Urol. 2016; 70(1):93-105.

2. Udager AM, Mehra R. Morphologic, molecular, and taxonomic evolution of renal cell carcinoma: a conceptual perspective with emphasis on updates to the 2016 World Health Organization classification. Arch Pathol Lab Med. 2016;140(10):1026–1037.

3. Xie L, Zhang Y, Wu CL. Microphthalmia family of transcription factors associated renal cell carcinoma. Asian J Urol. 2019 Oct;6(4):312-320.

4. Kmetec A, Jeruc J. Xp 11.2 translocation renal carcinoma in young adults; recently classified distinct subtype. Radiol. Oncol. 2014;48:197–202.

5. Sukov WR., Hodge JC., Lohse CM. et al. TFE3 rearrangements in adult renal cell carcinoma: Clinical and pathologic features with outcome in a large series of consecutively treated patients. Am. J. Surg. Pathol. 2012; 36:663–670.

6. Wyvekens N, Rechsteiner M, Fritz C et al. Histological and molecular characterization of TFEB-rearranged renal cell carcinomas. Virchows Arch. 2019; 474(5):625-631.

7. Sardiello M, Palmieri M, di Ronza A et al. A gene network regulating lysosomal biogenesis and function. Science 2009; 325(5939):473-7.

8. Perera RM, Stoykova S, Nicolay BN et al. Transcriptional control of autophagy-lysosome function drives pancreatic cancer metabolism. Nature. 2015; 524(7565):361-5.

9. Degenhardt K, Mathew R, Beaudoin B et al. Autophagy promotes tumor cell survival and restricts necrosis, inflammation, and tumorigenesis. Cancer Cell. 2006; 10(1):51-64.

10. Kauffman EC, Ricketts CJ, Rais-Bahrami S et al. Molecular genetics and cellular features of TFE3 and TFEB fusion kidney cancers. Nat Rev Urol. 2014; (8):465-75.

11. Davis IJ, Hsi BL, Arroyo JD et al. Cloning of an Alpha-TFEB fusion in renal tumors harboring the t(6;11)(p21;q13) chromosome translocation. Proc. Natl. Acad. Sci. USA 2003; 100, 6051-6056.

12. Kuiper RP, Schepens M, Thijssen J, Van Asseldonk M et al. Upregulation of the transcription factor TFEB in t(6;11)(p21;q13)-positive renal cell carcinomas due to promoter substitution. Hum. Mol. Genet. 2003; 1661-1669.

13. Caliò A, Segala D, Munari E, Brunelli M, Martignoni G. MiT Family Translocation Renal Cell Carcinoma: from the Early Descriptions to the Current Knowledge. Cancers (Basel). 2019 Aug 3;11(8):1110.

14. Argani P, Hawkins A, Griffin CA, et al. A distinctive pediatric renal neoplasm characterized by epithelioid morphology, basement membrane production, focal HMB45 immunoreactivity, and t(6;11)(p21.1;q12) chromosome translocation. Am J Pathol. 2001; 158:2089–2096.

15. Peckova K, Vanecek T, Martinek P et al. Aggressive and nonaggressive translocation t(6;11) renal cell carcinoma: comparative study of 6 cases and review of the literature. Ann Diagn Pathol. 2014; 18(6):351-7.

16. Smith NE, Illei PB, Allaf M, Gonzalez N, Morris K, Hicks J, Demarzo A, Reuter VE, Amin MB, Epstein JI, Netto GJ, Argani P. t(6;11) renal cell carcinoma (RCC): expanded immunohistochemical profile emphasizing novel RCC markers and report of 10 new genetically confirmed cases. Am J Surg Pathol. 2014 May;38(5):604-14.

17. Caliò A, Harada S, Brunelli M, Pedron S, Segala D, Portillo SC, Magi-Galluzzi C, Netto GJ, Mackinnon AC, Martignoni G. TFEB rearranged renal cell carcinoma. A clinicopathologic and molecular study of 13 cases. Tumors harboring MALAT1-TFEB, ACTB-TFEB, and the novel NEAT1-TFEB translocations constantly express PDL1. Mod Pathol. 2021 Apr;34(4):842-850.

18. Durinck S, Stawiski EW, Pavía-Jiménez A, et al. Spectrum of diverse genomic alterations define non-clear cell renal carcinoma subtypes. Nat Genet. 2015; 47(1):13-21.

19. Lilleby W, Vlatkovic L, Meza-Zepeda LA et al. Translocational renal cell carcinoma (t(6;11)(p21;q12) with transcription factor EB (TFEB) amplification and an integrated precision approach: a case report. J Med Case Rep. 2015; 9:281.

20. Cancer Genome Atlas Research Network, Linehan WM, Spellman PT, et al. Comprehensive Molecular Characterization of Papillary Renal-Cell Carcinoma. N Engl J Med. 2016; 374(2):135-145.

21. Argani P, Reuter VE, Zhang L, et al. TFEB-amplified Renal Cell Carcinomas: An Aggressive Molecular Subset Demonstrating Variable Melanocytic Marker Expression and Morphologic Heterogeneity. Am J Surg Pathol. 2016; 40(11):1484-1495.

22. Qu X, Tretiakova MS, Chen Y et al. TFEB amplification renal cell carcinoma detected by chromosome genomic array testing: A case report for diagnosis of a novel entity. J Clin Mol Pathol 2017; 2:7.

23. Williamson SR, Grignon DJ, Cheng L, et al. Renal Cell Carcinoma With Chromosome 6p Amplification Including the TFEB Gene: A Novel Mechanism of Tumor Pathogenesis?. Am J Surg Pathol. 2017; 41(3):287-298.

24. Gupta S, Johnson SH, Vasmatzis G, et al. TFEB-VEGFA (6p21.1) co-amplified renal cell carcinoma: a distinct entity with potential implications for clinical management. Mod Pathol. 2017; 30(7):998-1012.

25. Mendel L, Ambrosetti D, Bodokh Y, et al. Comprehensive study of three novel cases of TFEB-amplified renal cell carcinoma and review of the literature: Evidence for a specific entity with poor outcome. Genes Chromosomes Cancer. 2018; 57(3):99-113.

26. Mayoral Guisado C, Gómez Durán Á, Agustín Benítez López D, et al. Carcinoma de células renales asociado a amplificación del gen TFEB. Presentación de un caso y revisión de la literatura [TFEB-amplified renal cell carcinoma. A case report and review of the literature]. Rev Esp Patol. 2018; 51(4):248-252.

27. Martin EE, Mehra R, Jackson- Cook C, Smith SC. Renal cell carcinoma With TFEB translocation versus unclassified renal cell carcinoma with TFEB amplification. AJSP Rev Rep. 2017;22:305- 312.

28. Skala SL, Xiao H, Udager AM, et al. Detection of 6 TFEB-amplified renal cell carcinomas and 25 renal cell carcinomas with MITF translocations: systematic morphologic analysis of 85 cases evaluated by clinical TFE3 and TFEB FISH assays. Mod Pathol. 2018; 31(1):179-197.

29. Caliò A, Brunelli M, Segala D, et al. VEGFA amplification/increased gene copy number and VEGFA mRNA expression in renal cell carcinoma with TFEB gene alterations. Mod Pathol. 2019; 32(2):258-268.

30. Kojima F, Kuroda N, Matsuzaki I, et al. Aggressive TFEB-rearranged renal cell carcinoma mimicking chromophobe and clear cell renal cell carcinoma. Pathol Int. 2019; 69(1):51-53.

31. Wyvekens N, Rechsteiner M, Fritz C, et al. Histological and molecular characterization of TFEB-rearranged renal cell carcinomas. Virchows Arch. 2019; 474(5):625-631.

32. Gupta S, Argani P, Jungbluth AA, et al. TFEB Expression Profiling in Renal Cell Carcinomas: Clinicopathologic Correlations. Am J Surg Pathol. 2019; 43(11):1445-1461.

33. Vormittag-Nocito E, Matrova E. A unique case of TFEB amplified renal cell carcinoma. Pathology. 2020; 52(6):727-729.

34. Kammerer-Jacquet SF, Deleuze A, Saout J, Mathieu R, Laguerre B, Verhoest G, Dugay F, Belaud-Rotureau MA, Bensalah K, Rioux-Leclercq N. Targeting the PD-1/PD-L1 Pathway in Renal Cell Carcinoma. Int J Mol Sci. 2019 Apr 4;20(7):1692.

35. Krigsfeld GS, Prince EA, Pratt J, Chizhevsky V, William Ragheb J, Novotny J Jr, Huron D. Analysis of real-world PD-L1 IHC 28-8 and 22C3 pharmDx assay utilisation, turnaround times and analytical concordance across multiple tumour types. J Clin Pathol. 2020 Oct;73(10):656-664.

36. Kammerer-Jacquet SF, Crouzet L, Brunot A, et al. Independent association of PD-L1 expression with noninactivated VHL clear cell renal cell carcinoma-A finding with therapeutic potential. Int J Cancer. 2017;140(1):142-148.

37. Gowrishankar B, Przybycin CG, Ma C, et al. A genomic algorithm for the molecular classification of common renal cortical neoplasms: development and validation. J Urol. 2015;193(5):1479-1485.

38. Leibovich BC, Sheinin Y, Lohse CMet al. Carbonic anhydrase IX is not an independent predictor of outcome for patients with clear cell renal cell carcinoma. J Clin Oncol 2007; 25: 4757–4764.

39. Myllykangas S, Bohling T, Knuutila S, et al. Specificity, selection and significance of gene amplifications in cancer. Semin Cancer Biol. 2007; 17:42–55.

40. Settembre C, Di Malta C, Polito VA, et al. TFEB links autophagy to lysosomal biogenesis. Science 2011; 332(6036): 1429–1433.

41. Martina JA, Diab HI, Lishu L, et al. The nutrient-responsive transcription factor TFE3 promotes autophagy, lysosomal biogenesis, and clearance of cellular debris. Sci Signal 2014; 7(309): ra9.

42. Steingrimsson E, Tessarollo L, Pathak B, et al. Mitf and Tfe3, two members of the Mitf-Tfe family of bHLH-Zip transcription factors,have important but functionally redundant roles in osteoclast development. Proc Natl Acad Sci U S A 2012; 99(7): 4477–4482.

43. Settembre C, Zoncu R, Medina DL, et al. A lysosome-to-nucleus signalling mechanism senses and regulates the lysosome via mTOR and TFEB: Self-regulation of the lysosome via mTOR and TFEB. EMBO 2012; 31(5): 1095–1108.

44. Roczniak-Ferguson A, Petit CS, Froehlich F, et al. The Transcription Factor TFEB Links mTORC1 Signaling to Transcriptional Control of Lysosome Homeostasis. Sci Signal 2012; 5(228): ra42-ra42.

45. Di Malta C, Ballabio A. TFEB-mTORC1 feedback loop in metabolism and cancer. Cell Stress. 2017; 1(1):7-10. Published 2017 Oct 1.

46. Yang J, Yang D, Sun Y, et al. Genetic amplification of the vascular endothelial growth factor (VEGF) pathway genes, including VEGFA, in human osteosarcoma. Cancer 2011;117:4925–4938.

47. Trinh, X., Tjalma, W., Vermeulen, P. et al. The VEGF pathway and the AKT/mTOR/p70S6K1 signalling pathway in human epithelial ovarian cancer. Br J Cancer 2009 ; 100, 971–978.

48. Zhang C, Duan Y, Xia M, et al. TFEB Mediates Immune Evasion and Resistance to mTOR Inhibition of Renal Cell Carcinoma via Induction of PD-L1. Clin Cancer Res. 2019; 25(22):6827-6838.

TABLES

Table 1 Clinical features of TFEB-amplified renal cell carcinoma

Case	Age	Gender	Size (cm)	Type of nephrectomy	Stage TNM at diagnosis	Treatment	Follow up
1	58	M	20	Radical	pT2b Nx M1	Sunitinib (12 months) (radiologic progression) Cabozantinib (3 months) (progression non specified) mTOR inhibitor (16 months) (radiologic progression) Nivolumab (2 months) (no progression)	Synchronous liver metastasis, alive at 53 months
2	31	M	10	Radical	pT3b Nx M0	Laminectomy + radiotherapy Sunitinib (1 month) (bone metastasis progression) Nivolumab (5 months) (no progression)	Bone metastasis at 4 months, alive at 14 months
3	72	M	3	Partial	pT1a Nx M0	Palliative care	Lung, liver and adrenal gland metastasis at 29 months, death at 36 months
4	62	F	12.5	Radical	pT3a N0 M0	na	Alive at 18 months
5	47	M	15.5	Radical	pT3a N0 M0	Lymph node dissection. No systemic treatment.	Lymph node metastasis at 16 monhs, alive at 43 months
6	72	M	4.3	Partial	pT3a N0 M0	na	Alive at 24 months
7	38	M	10	Radical	pT3a Nx Mx	na	na
8	86	M	5.5	None	cpT2a N1 Mx	Palliative care	Synchronous lymph node metastasis, rapid death
9	70	F	8.4	Radical	pT3a Nx Mx	na	na

na : non available

Table 2 Pathological features of TFEB-amplified renal cell carcinoma

Case	Size (cm)	Stage TNM	ISUP	Architecture	Cytology	Necrosis	Original diagnosis
1	20	pT2b Nx M1	3	Solid and papillary architecture	Eosinophilic cells	no	Oncocytoma
2	10	pT3b Nx M0	3	Trabecular	Eosinophilic cells, prominent nucleoli	yes	Papillary RCC
3	3	pT1a Nx M0	4	Solid and trabecular	Eosinophilic and clear cells, prominent nucleoli	yes	Clear cell RCC
4	12.5	pT3a N0 M0	3	Trabecular and alveolar	Clear and eosinophilic cells	yes	Unclassified
5	15.5	pT3a N0 M0	3	Trabecular and papillary	Eosinophilic and clear cells	yes	Unclassified
6	4.3	pT3a N0 M0	3	Solid	Eosinophilic cells, prominent nucleoli	no	Oncocytoma
7	10	pT3a Nx Mx	3	Tubulo-papillary	Eosinophilic cells, prominent nucleoli	yes	Papillary RCC
8	5.5	cpT2a N1 Mx	3	Solid	Eosinophilic and clear cells	no	Unclassified
9	8.4	pT3a Nx Mx	4	Solid or papillary	Clear and eosinophilic cells, prominent nucleoli	yes	Unclassified

Table 3 Immunohistochemistry in TFEB-amplified renal cell carcinoma

Case	PAX8	CD117	Melan-A	HMB45	CD10	CA IX	CK07	TFE3	AMACR	PD1	PDL1	CD8
1	+ (10%)	+ (80%)	+ (60%)	+ (5%)	-	-	-	-	+ (60%)	na	na	na
2	+ (50%)	-	+ (10%)	+ (5%)	-	+ (10%)	-	-	+ (100%)	2	80	2
3	+ (80%)	+ (10%)	+ (40%)	+ (2%)	+ (70%)	+ (5%)	+ (5%)	-	+ (10%)	1	30	2
4	+ (50%)	-	+ (10%)	-	-	-	+ (10%)	-	+ (90%)	2	70	3
5	+ (10%)	-	+ (80%)	-	+ (80%)	-	+ (5%)	-	+ (10%)	1	10	1
6	+ (60%)	-	+ (10%)	-	+ (10%)	+ (5%)	-	-	+ (90%)	1	5	1
7	+ (90%)	+ (10%)	+ (10%)	-	+ (80%)	+ (10%)	-	-	+ (100%)	1	30	2
8	+ (70%)	+ (10%)	+ (80%)	+ (5%)	+ (60%)	+ (10%)	+ (10%)	-	+ (90%)	na	na	na
9	+ (80%)	-	+ (30%)	+ (5%)	+ (10%)	-	-	-	+ (70%)	1	0	3

na : non available

Table 4 FISH results in TFEB-amplified renal cell carcinoma

Cases	High or low level of *TFEB* amplification	Concomitant *TFEB* rear-rangement	Deletion of *VHL*	Chromosomes 7 and 17
1	high	no	na	na
2	low	no	yes	no
3	high	no	yes	no
4	high	no	na	na
5	high	yes	na	na
6	high	no	na	na
7	low	no	na	na
8	high	no	na	na
9	low	no	na	na

na : non available

Table 5 Chromosomic alterations in TFEB-amplified renal cell carcinoma

Cases	Gains	Losses
Case 1	+1q, +6p, +8p, +8q, +10, +17q	-1p, -2q, -5, -6p, -8p, -8q, -13, -14, -18, -Y
Case 2	+6p, +8p, +8q, +9p	-3p (*VHL*), -4q, -6p, -6q, -8p, -9p, -11p, -13q, -17p, -18q
Case 3	+6q, +6p	-1p, -2q, -3p (*VHL*), -6p, -6q, -9p, -12p, -16q, -18q, -19q
Case 4	+1q, +2q, +8, +16, +20	-2q, -6p
Case 5	+1q, +6q	-1p, -2q, -3 (*VHL*), -6p, -19q, -22
Case 6	+6p, +7p, +8p, +8q, +17q	-1p, -2q, -8p, -8q, -10q, -15q, -17p, -18, -21q, -22q
Case 7	+4p, +4q, +6p, +17q	-1p, -2q, -3p (*VHL*), -4p, -4q, -6p, -17p, -18q, -19p, -21, -22
Case 8	+5p, +5q, +7, +8p, +8q, +13q, +18q, +19p, +20, +X	-1p, -2q, -5q, -6p, -6q, -13q, -19p, -Y
Case 9	+6p	-1p, -3p (*VHL*), -3q, -9, -13, -18, -22

FIGURES LEGENDS

Figure 1: Representative histological features of *TFEB*-amplified RCC. A, solid and cribriform architecture with central necrosis (case 2); B, solid and alveolar architecture with eosinophilic tumor cells (case 6); C, papillary architecture (case 7); D, tumor cells with microvascular cytoplasm (case 9); E, solid architecture with clear cell component (case 3); F, microcystic and alveolar architecture (case 1).

Figure 2: Immunohistochemistry. A, focal positivity of Melan-A (case 9); B, rare positivity of HMB45 (case 8); C, nuclear expression of PAX8 (case 3); D, diffuse positivity of AMACR (case 6); E, expression of CAIX at the edge of necrosis area (case 7), F, diffuse expression of PDL1 (case 2).

Figure 3: A, Array-CGH showing complex quantitative whole genome profile : losses of chromosome segments 1p, 2q, 3p, 4p, 4q, 6p, 17p, 18q, 19p and whole chromosomes 21 and 22 and gains of chromosome segments 4p, 4q, 6p and 17q, including amplification of *TFEB* gene at 6p21.1; B, zoom on chromosome 6 and *TFEB* amplification; C, interphase FISH analysis using a *TFEB* break-apart probe, showing amplification of *TFEB* (more than 5 copies of non-rearranged TFEB/cell).

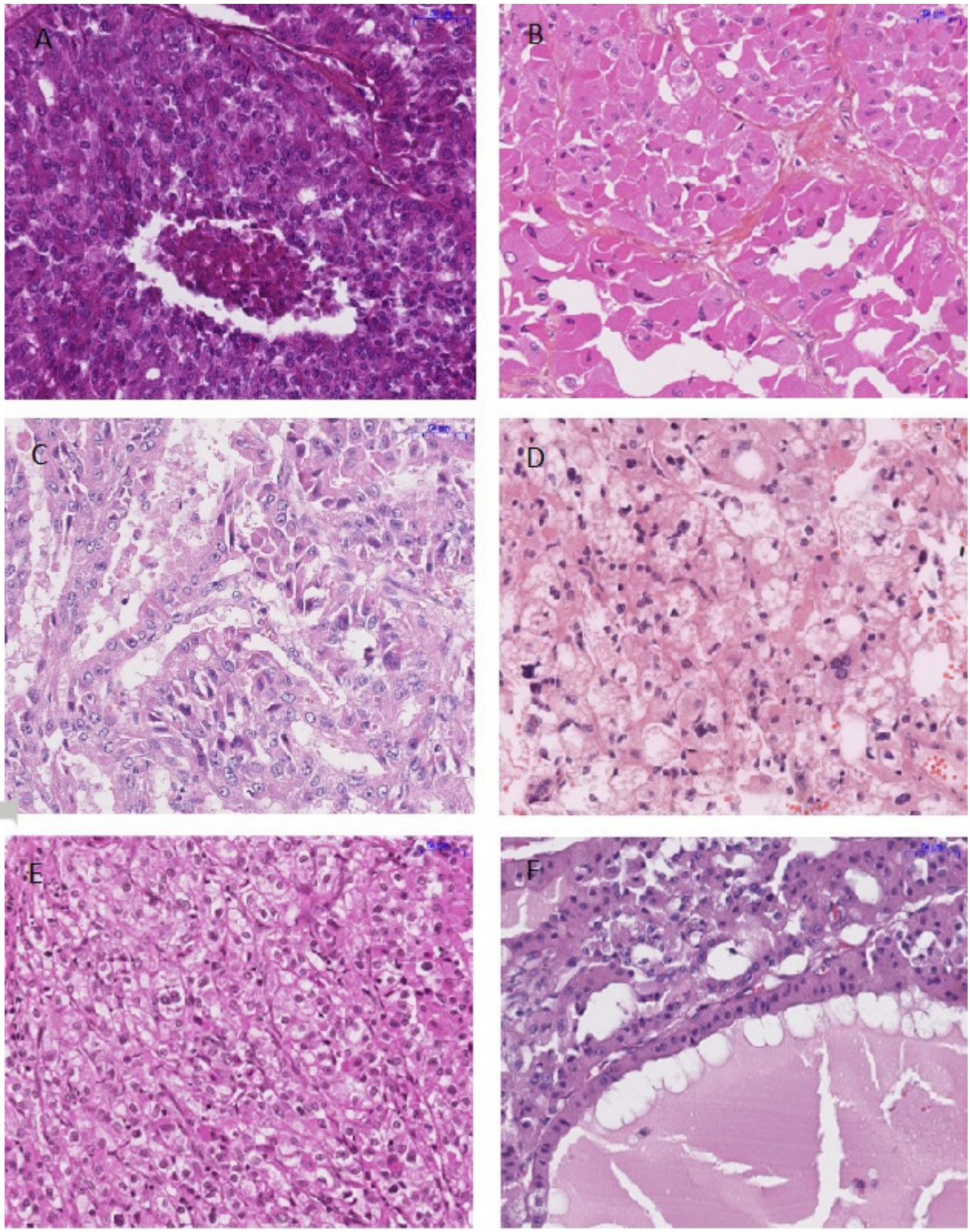

HIS_14683_Figure_1_JPEG.jpg

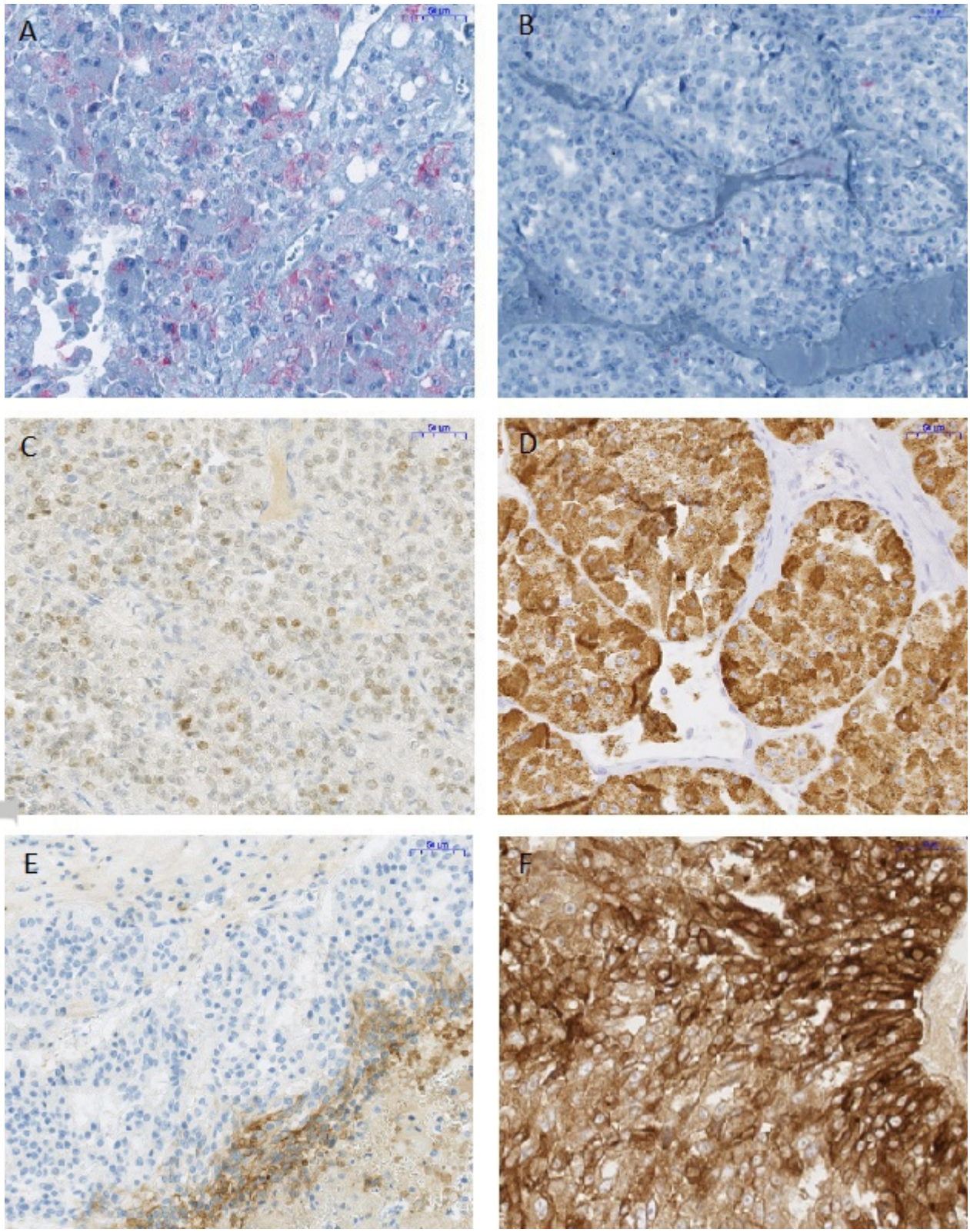

HIS_14683_Figure_2_JPEG.jpg

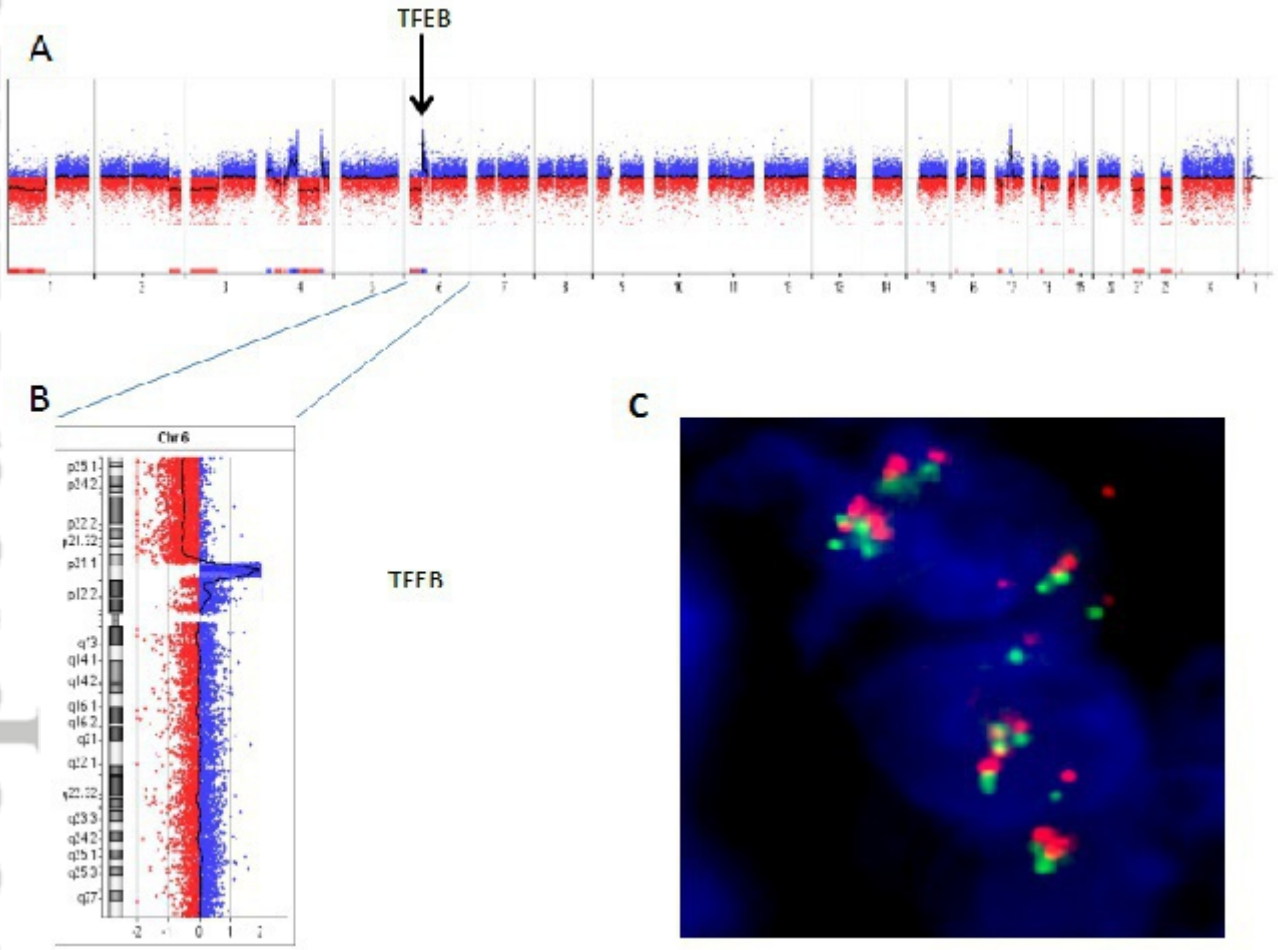

HIS_14683_Figure_3_JPEG.jpg